Available online at www.sciencedirect.com
ScienceDirect
Journal of Nuclear Materials 362 (2007) 309–315
journal of nuclear materials
www.elsevier.com/locate/jnucmat

High temperature creep properties of zirconium and Zircaloy-4 in vacuum and oxygen environments

G. Moulin, R. El Tahhan, J. Favergeon *, M. Bigerelle, M. Viennot

Laboratoire ROBERVAL, FRE CNRS 2833, Centre de Recherches de Royallieu, Université de Technologie de Compiègne, BP 20529, F-60205 Compiègne, France

Abstract

A special set-up has been used to follow the evolution of mechanical parameters under various applied stresses in in situ conditions (controlled temperature and atmosphere). This experimental set-up is used to study the creep behavior of zirconium and Zircaloy-4 in the temperature range 723–823 K. The influence of applied stresses, atmosphere and alloy grade on the deformation and oxidation processes are specifically analyzed. The results underline the presence of two distinct deformation domains for both alloy grades, depending on the applied stress value and the temperature. The results show that the presence of an oxide scale only leads to slight modifications of the creep behavior.

PACS: 47.54.Jk; 46.35.+z

1. Introduction

High temperature oxidation of pure zirconium and zirconium alloys is very sensitive to many metallurgical, physico-chemical and mechanical factors. In industrial applications, high temperature is usually combined with applied stresses, which leads to creep deformation.

Generally, the creep of materials comprises three successive domains:

- The primary creep where the specimen begins to deform relatively quickly whereupon the creep rate decreases with time.
- The secondary creep which is characterised by a constant strain rate.
- The tertiary creep which corresponds to an increase of the strain rate and finally leads to the failure of the material.

At high temperature, there are two kinds of creep mechanism: creep controlled by dislocation movements, and creep controlled by diffusion. For the first kind, when the plastic flow is mainly ensured by the thermally activated movement of dislocations, creep follows a power law of the Norton type [1]:

$$\dot{\varepsilon} = A\sigma_0^n \exp\left(-\frac{\Delta E}{RT}\right), \tag{1}$$

where $\dot{\varepsilon}$ is the strain rate, σ_0 is the applied stress, A and n are constants, ΔE is the molar activation

* Corresponding author. Tel.: +33 3 44 23 45 33; fax: +33 3 44 23 49 84.
E-mail address: jerome.favergeon@utc.fr (J. Favergeon).

0022-3115/$ - see front matter © 2007 Elsevier B.V. All rights reserved.
doi:10.1016/j.jnucmat.2007.01.080

enthalpy, R the gas constant and T is the absolute temperature.

When creep is controlled by core diffusion, the power-law does not apply anymore and the strain rate is a function of the applied stress, σ_0, the vacancies diffusion coefficient, D, and the grain size, d. In the case of core diffusion (Nabarro–Herring creep) [2], the strain rate, $\dot{\varepsilon}$, is given by [3]:

$$\dot{\varepsilon} = K\frac{\sigma_0 D}{d^2}\exp\left(-\frac{\Delta E}{RT}\right), \quad (2)$$

where K is a constant.

The levels of applied stress and temperature used in the present study should normally lead to dislocation-controlled creep of zirconium and Zircaloy-4 [4,5]. So the analysis of the creep results will focus on power-law creep (Eq. (1)).

The purpose of this paper is to quantify the effect of an oxide scale on the creep behavior of zirconium and Zircaloy-4. In order to accelerate the experiments and to obtain sufficiently thick oxide scales, the creep temperatures are chosen in the range 723–823 K. These temperatures are higher than the operating temperatures used in the nuclear industry. But the applied stress values are chosen to yield similar creep mechanisms as in the normal operating conditions.

2. Materials and experiments

The materials used in this work are cold rolled zirconium from Goodfellow and cold rolled Zircaloy-4 from Cezus. The chemical compositions of these materials are given in Table 1. Both metals exhibit the classical rolled texture of zirconium alloys which corresponds to a misorientation of the basal plane (0 0 1) of 30° as referred to the sample surface. The as-received plates are machined to form test-plates with a rectangular useful length of 12 mm in the rolled direction and a thickness of 1 mm. The width of the test-plates is 2 mm. After cutting, the test-tubes are first polished with abrasive paper (SiC) until grade 2500 followed by a 'polished mirror' with OPS solution (suspension of colloidal silica). The sample is then cleaned and dried. After polishing, the samples are annealed during 5 h under primary vacuum at 973 K to stabilize the microstructure and to remove the residual stresses. Finally the surface is polished again with a felt cloth and OPS solution.

The creep tests were performed in a special set-up (Fig. 1) which allows to apply micro-deformations (a few μm) or to impose loads on the samples. In the present study, the set-up has been configured to perform uniaxial sollicitations. Note that the configuration can be switched to a four point bending geometry. The sample is fixed between two tongs (one is mobile, the other one is fixed), at the end of an alumina cane. This cane is then introduced into a quartz tube which is hermetically closed and connected to a primary vacuum pump. The atmosphere within the quartz tube can be modified using a source of dry $^{16}O_2$ or an $^{18}O_2$ tank. This tank is a container of zeolite which traps oxygen when it is at low temperature. To release oxygen 18 and inject it into the quartz tube, it is thus necessary to heat the tank. After a test, oxygen 18 is recovered by cooling the tank with liquid nitrogen. Another reserve of this type is used to trap the remaining impurities after pumping to improve the vacuum. The pressure in the enclosure is measured using a primary vacuum gauge. The temperature around the sample is controlled with a furnace which slides around the quartz tube. The maximum temperature of the sample could be 1273 K.

The displacement of the moving tong is ensured by a small engine controlled by a computer and located outside the assembly. Still outside the assembly, there are force and displacement sensors, and acoustic emission sensors which allow the detection of the acoustic signal emitted by the sample and transmitted through the alumina cane which is used as a wave guide. It is thus possible to follow, in situ, the evolution of the force, the displacement and the mechanical damages in temperature under mechanical sollicitation and controlled atmosphere. To obtain the creep behavior of zirconium and Zircaloy-4, the test-plates are heat treated for 4 h under controlled temperature ($723 < T < 823$ K), and under controlled atmosphere (primary vacuum

Table 1
Chemical composition of zirconium and Zircaloy-4 in weight %

	Sn	Fe	Cr	Ni	Hf	O	C	N	H	Zr
Zr	–	0.02	0.020	–	0.250	0.10	0.025	0.01	0.001	Bal
Zry-4	1.34	0.22	0.110	0.004	0.0044	0.120	0.0119	0.0034	<0.0003	Bal

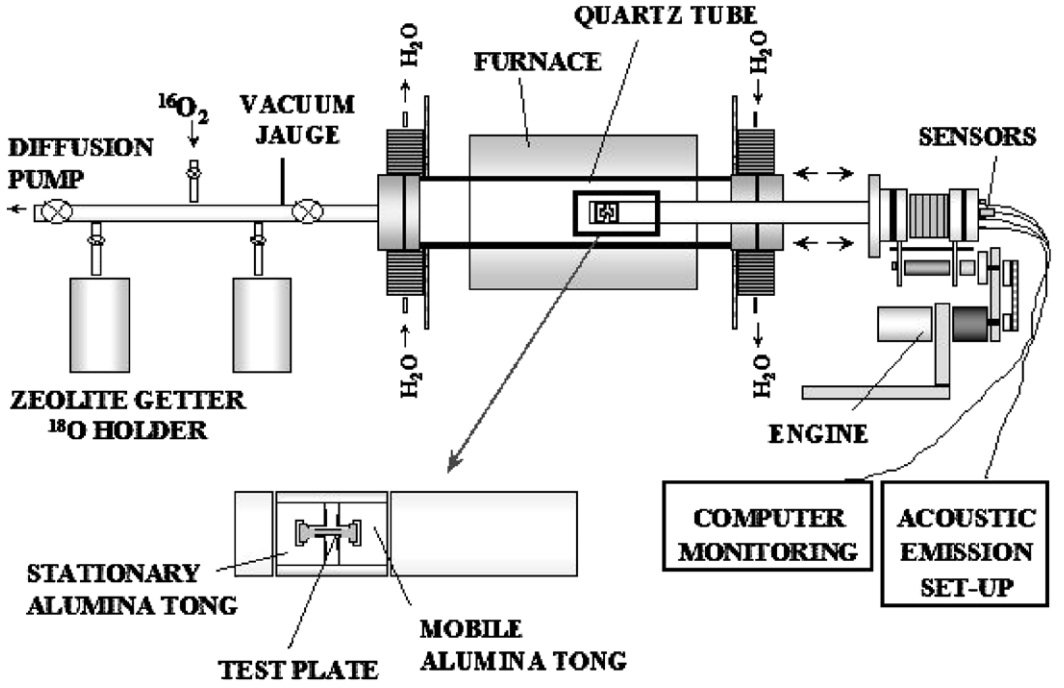

Fig. 1. Scheme of the experimental set-up used in the present study for the creep experiments under controlled atmosphere.

with $P = 10^{-1}$ Pa, or dry $^{16}O_2$ with a pressure of 10^5 Pa). Then the samples, which are covered by an oxide film when the experiments are performed under dry oxygen, are submitted for 3 h to a constant applied stress, σ_0. During this 3 h creep experiment, when an oxidant atmosphere is used, the dry oxygen $^{16}O_2$ is replaced by $^{18}O_2$ ($P = 2 \times 10^3$ Pa) after 1 h of creep to perform later study of the oxygen diffusion in the oxide scales under creep conditions. Finally, a relaxation step is performed with constant elongation for 1 h without changing the atmospheric conditions. Force and displacement are recorded during the whole experiment, as the acoustic emission signals, which give information on the mechanical damages of the specimen.

3. Results

3.1. Thicknesses of the oxide scales

After complete experiments, the oxide thicknesses are measured by microscopic observations of specimen cross-sections. For experiments conducted under reduced pressure, very thin oxide scales (a few nanometers thick) are observed. When the experiments are performed under oxidant atmosphere, the thickness of the scale is more significant. Fig. 2 gives one part of the measured thicknesses obtained on zirconium and Zircaloy-4 after 773 K experiments under various applied stresses, σ_0, and under oxidant atmosphere. The thickness values are given with a standard uncertainty of ± 0.1 μm. One notes that the final oxide thickness of the oxide scales depends on the nature of the material: Zircaloy-4 generally exhibits thicker oxide scales on the surface than zirconium. This thickness also depends on the value of the applied stress in creep:

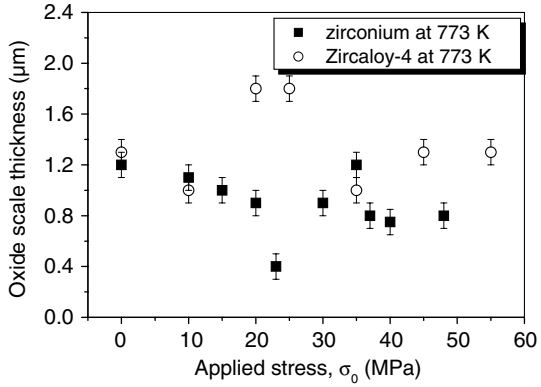

Fig. 2. Oxide thickness measured after the creep tests against the applied stress, σ_0, for zirconium and Zircaloy-4 at 773 K under oxidant atmosphere.

the thickness of the scale tends to decrease with the applied stress for zirconium. For Zircaloy-4, the evolution of the oxide thickness with the applied stress is much more difficult to qualify. Note that a dependance of the oxygen diffusion coefficient in the zirconia scales has been shown [6] with the applied stress in creep because it modifies the activation energy for oxygen diffusion. Even if the zirconia growth rate is controlled by the oxygen diffusion in the case of zirconium and Zircaloy-4, the creep behavior also affects the density of the scales and so the concentration of vacancies which take part in the limiting-rate diffusion process. Then data of the oxygen diffusion coefficient dependency with applied stress (as reported in [6]) are not sufficient to obtain the relation between the growth rate of the scales and the creep rate of the metal/oxide system.

However, when using oxidant atmosphere, one considers that the differences of oxide scale thicknesses between the different experiment conditions are small enough to be neglected.

3.2. Creep experiments

Fig. 3 presents the elongation of the samples, which are recorded as a function of time, for the oxidized zirconium at different temperatures under a 20 MPa applied stress. These curves exhibit a first domain at the beginning when the creep rate decreases with time; this is the primary creep domain. Then elongation varies linearly with time: this is the secondary creep domain. From these data, linearisations are performed for the secondary creep domain, and the obtained slopes correspond to the steady state creep rates of the specimens, $\dot{\varepsilon}_s$. The creep rates are plotted against the applied stress, σ_0, in log–log diagrams in order to determine the Norton exponent, n, from Eq. (1). These graphs exhibit two successive linear parts that correspond to two different creep behaviors, regardless of the temperature, the material and the atmosphere (see Fig. 4(a) and (b) as examples of the obtained graphs). The n exponent values are summarized in Table 2 for the different tests performed during this study; for each case, the n_l and n_h values refer to the

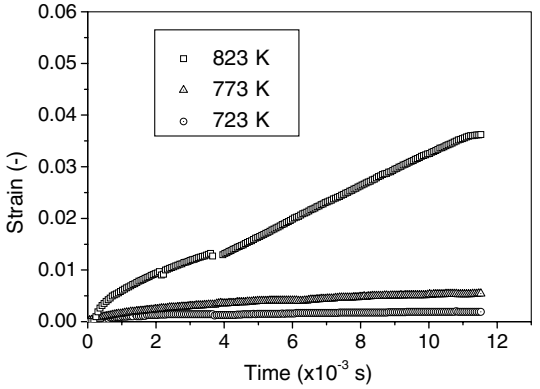

Fig. 3. Plot of strain against time for creep tests of zirconium at 723, 773 and 823 K under oxygen for applied stress of $\sigma_0 = 20$ MPa.

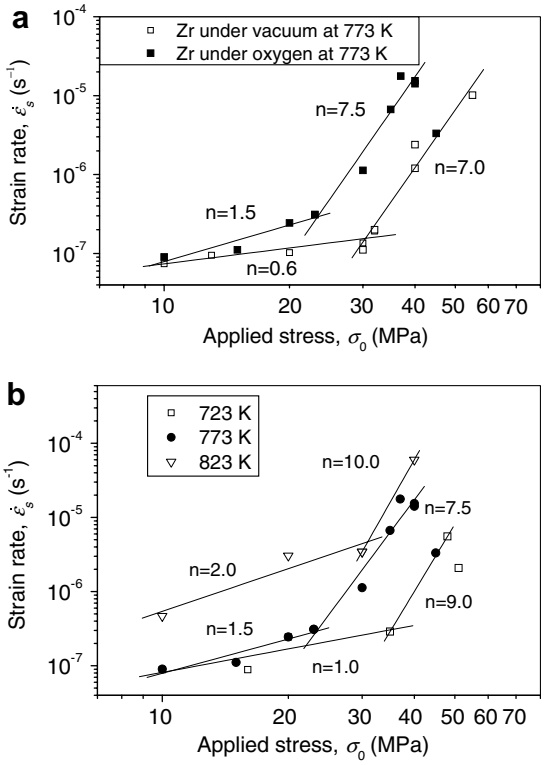

Fig. 4. Plot of the logarithm of strain rate, $\dot{\varepsilon}_s$, against the logarithm of the applied stress, σ_0, for zirconium: (a) at 773 K under vacuum and under oxygen; (b) at 723, 773 and 823 K under oxygen.

Table 2
Reported exponents of the Norton law obtained from the creep curves – For each case, n_l and n_h represents the exponent of the low and high applied stress domains respectively

	Zirconium				Zircaloy-4			
	Vacuum		Oxygen		Vacuum		Oxygen	
T (K)	n_l	n_h	n_l	n_h	n_l	n_h	n_l	n_h
723	–	–	1.0	9.0	–	–	0.6	3.5
773	0.6	7.0	1.5	7.5	0.2	5.0	0.4	9.0
823	–	–	2.0	10.0	–	–	–	–

Table 3
Values of the critical applied stress, $\sigma_{0,c}$, which separates the low and the high applied stress domains in the creep curves

	Zirconium $\sigma_{0,c}$ (MPa)		Zircaloy-4 $\sigma_{0,c}$ (MPa)	
T (K)	Vacuum	Oxygen	Vacuum	Oxygen
723	–	35	–	40
773	30	25	45	40
823	–	30	–	–

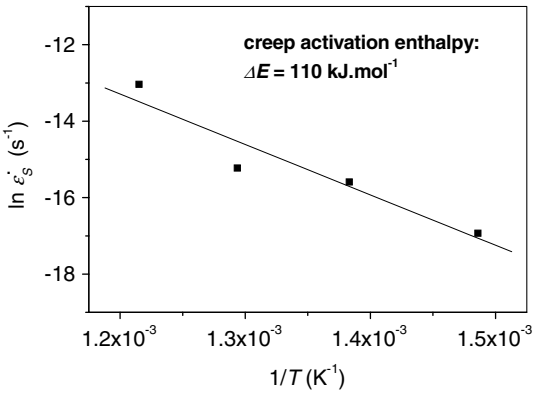

Fig. 5. Plot of the natural logarithm (ln) of the strain rate, $\dot{\varepsilon}_s$, against the reciprocal of the absolute temperature, $1/T$, to determine the activation energy for the oxidized zirconium under an applied stress of 20 MPa.

n exponent of the low and high applied stress regime respectively. Table 3 gives the critical values of the applied stress that denote the limit between the low and high applied stress creep regime.

Taking the steady state creep rates, $\dot{\varepsilon}_s$, for a given material, atmosphere and applied stress, σ_0, but at different temperatures, the plot of $\ln \dot{\varepsilon}_s$ as a function of $1/T$ allows determination of the activation energy, ΔE, of the Norton law (Eq. (1)) – see Fig. 5. Table 4 summarizes the activation energies obtained for the applied stresses, σ_0, equals to 20 and 40 MPa and for oxidized zirconium and Zircaloy-4 samples.

3.3. Relaxation experiments

After the creep tests, the elongation is maintained constant and the stress is recorded as a function of time. The relaxation results obtained at 723 K for oxidized and unoxidized zirconium and Zircaloy-4 are presented in Fig. 6. From such results, one can define the released stress, $\Delta\sigma$, and the remaining internal stress, σ_i, as shown in Fig. 7. For such an analysis, the first part of the relaxation curve is simulated by a logarithmic law. The released stress, $\Delta\sigma$, is then defined by the difference between the initial stress, σ_0, and the final stress of the logarithmic domain, σ_f. For the second part of the relaxation curves, a hyperbolic law can be fitted to the experimental data. Even if creep tests are too short to be sure that the stress stops decreasing at the end of the experiments, the fitting functions show that later decrease of the stress should be very low. So the remaining internal stresses, σ_i, obtained with these experiments are good approximations.

As an example, the released stress, $\Delta\sigma$, and internal stress, σ_i, are reported as a function of the applied stress in Fig. 8 for oxidized and unoxidized Zircaloy-4 at 773 K. Comparing the released stress

Table 4
Creep activation molar enthalpies, ΔE, of oxidized zirconium and Zircaloy-4 for two different applied stress values, 20 and 40 MPa

Applied stress σ_0 (MPa)	Zirconium ΔE (kJ mol^{-1})	Zircaloy-4 ΔE (kJ mol^{-1})
20	110	103
40	97	48

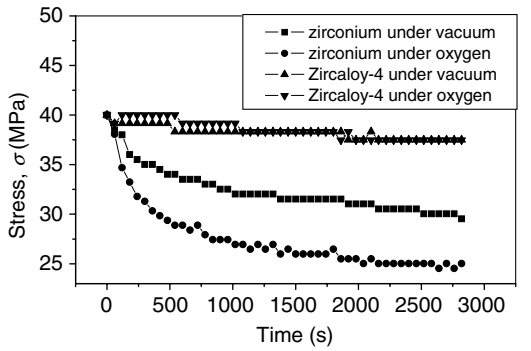

Fig. 6. Plot of stress against time during relaxation experiments at constant elongation after a 40 MPa creep experiment, for zirconium and Zircaloy-4, under vacuum or oxygen, at 773 K.

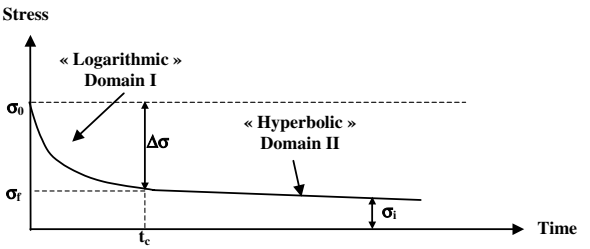

Fig. 7. Sketch of the plot obtained from relaxation experiments, showing the definition of the released stress, $\Delta\sigma$, and of the internal stress, σ_i.

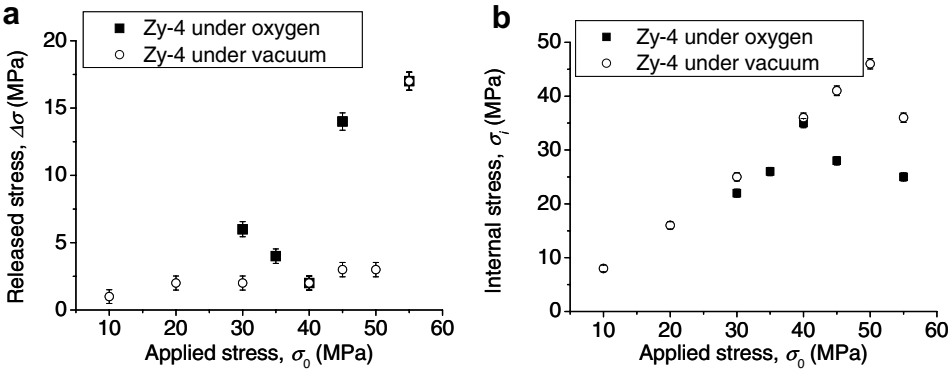

Fig. 8. Evolution of the released stress, $\Delta\sigma$, (a) and of the internal stress, σ_i, (b) against the applied stress, σ_0, after creep at 773 K for oxidized and unoxidized Zircaloy-4.

under vacuum (without oxide scale) and under oxygen (with an oxide scale), one notes that the evolution of $\Delta\sigma$ with the applied stress is more scattered when the metal is covered by zirconia. Moreover, when the oxide scale is present, we observe a big difference of the $\Delta\sigma$ values between the low stress domain ($\sigma_0 < 40$ MPa) and the high stress domain ($\sigma_0 \geqslant 40$ MPa) (Fig. 8(a)). Such a limit corresponds to the limit which has already been observed for the strain rates reported in Table 3.

For the internal stress, σ_i (Fig. 8(b)), there is a significant evolution according to the applied stress for the oxidized material; a break in this evolution is again observed around the same value of the applied stress as the break observed in the evolution of the relaxed stress.

All these observations are also valid for zirconium and at other temperatures (723 and 823 K) [7].

4. Discussion

The creep experiments show that for both zirconium and Zircaloy-4 the Norton law (Eq. (1)) is followed, regardless of the temperature and with or without an oxide scale on the surface. But, in the range of applied stress used, two distinct domains are always observed (Fig. 4(a) and (b)):

- The first domain corresponds to the lowest values of the applied stress, σ_0, and the n exponent of the Norton law lies between 0.2 and 2.0.
- For the highest applied stress values, the n exponent varies between 3.5 and 10.0.

In the literature, such differences of the n values between the two domains are connected to the mode of deformation (dislocation glide for the lowest values of applied stress and dislocation climb for the highest values) [4,8]. These two domains are clearly identified on Ashby's maps of standard deformation for zirconium [5] and for Zircaloy-2 [4]. It then appears that the presence of the oxide scale does not modify the mechanism of deformation of the metal but the zirconia layers only act on the creep rates and on the critical values of the applied stress that separate the two observed domains (Tables 2 and 3 – Fig. 4(a)): the oxide scale tends to accelerate the creep deformation (especially for the high stress regime). To explain this later observation, it is probably pertinent to take into account the stress distribution in the oxidized samples since the oxide is in compression because of growth stresses [9] and the substrate counter-reacts in tension to ensure mechanical continuity at the metal–oxide interface. So additional positive stress from the oxide layer helps to increase the applied tensile stress, σ_0, accelerating the deformation rate of the oxidized system [10].

The comparison of the creep behavior of zirconium and Zircaloy-4 shows that the creep rates are generally smaller in the case of Zircaloy-4, with or without an oxide scale on the surface. Such a behavior is probably due to the presence of tin in the Zircaloy-4 alloy.

Concerning the molar activation enthalpies for zirconium and Zircaloy-4, the values are respectively equal to 110 and 103 kJ mol^{-1} for a 20 MPa value of applied stress and 97 and 48 kJ mol^{-1} under 40 MPa. These values are of the same order as the energy of zirconium self-diffusion given by Gruzin et al. [11] which equals to 92 kJ mol^{-1}. It is interesting to note that these activation energies are weak

and not very different from one deformation mechanism to the other (dislocation climb or glide).

Concerning the stress relaxation results (Fig. 8(a)), it appears clearly that the released stress is essential when the material is covered by an oxide layer. Indeed this stress relaxation is almost equal to zero after creep under vacuum. It thus seems logical to conclude that the stress relaxation is due to the presence of the oxide scale and/or its interaction with the substrate.

We also note that the released stress, $\Delta\sigma$, remains small for the low applied stress values, but in the domain of high σ_0 values, $\Delta\sigma$ becomes more significant. This result would be well-explained if we consider undamaged oxide scales. But actually the oxide scales have a significant crack network after creep; they stay fully adherent to the substrate, except for the high applied stress values where the outer part of the scales spalls off. In this case, the thin inner scale can be quickly repaired by later oxidation which could then explain a high stress level in the scale (because of mechanical continuity with the metal) at the end of the creep step, which is then released.

With regard to the internal stress, σ_i, (Fig. 8(b)), which is strongly controlled by the substrate, there are no important modification between creep under vacuum and creep under oxygen in the low applied stress domain. On the other hand, when high stresses are applied, there is a significant fall of the σ_i values in the case of oxidized materials. This could be explained by an easy initiation and propagation of cracks at low applied stress values in the upper part of the oxide, and a propagation of these cracks into the metal at the highest applied stress values. This could lead to a softening of the oxidized system by significant cracking of the interfacial zone and of the upper part of the substrate [7]. This could also help with the movement and elimination of the dislocations in this area, where the dislocation density is very high.

5. Conclusion

The analysis of zirconium and Zircaloy-4 deformation under creep conditions between 723 and 823 K shows that the strain rates obey the Norton law. Two creep mechanisms exist for applied stress values lying in the range 10–55 MPa. The mechanism of low applied stress is controlled by dislocation glide. High applied stress values lead to a dislocation climb controlled mechanism. The presence of the oxide scale on the surface of the metallic substrate does not modify the creep mechanism. This oxide scale only modifies the values of the creep rates (they increase with the presence of the oxide scale) and the critical applied stress which delimits the two creep domains. The nature of the materials also leads to modification of the creep rates: the strain rates are generally higher for zirconium than for Zircaloy-4. The determination of the activation energies for the creep shows that the strain rates increase with temperature for both materials. The values obtained in the present study are in agreement with the literature data reported by Kaddour et al. [12].

Complementary relaxation experiments show that one part of the stress is released by the material at constant elongation after creep, and another part appears as an internal permanent stress. Such values are correlated to the mechanical damage that takes place in the sample (the damage analysis is presented in details in [7]).

References

[1] O. Golan, A. Arbel, D. Eliezer, D. Moreno, Mater. Sci. Eng. A A216 (1996) 125.
[2] R. Raj, M.F. Ashby, Met. Trans. 2 (1971) 1113.
[3] M.F. Ashby, D.R.H. Jones, 2nd ed., Engineering Materials, Vol. 1, Butterworth and Heinemann, 1996, p. 174.
[4] D.B. Knorr, M.R. Notis, J. Nucl. Mater. 56 (1975) 18.
[5] P.M. Sargent, M.F. Ashby, Scr. Metall. 16 (1982) 1415.
[6] R. El Tahhan, G. Moulin, M. Viennot, J. Favergeon, P. Berger, Mater. Sci. Forum 461–464 (2004) 783.
[7] R. El Tahhan, Interactions entre la sollicitation mécanique en fluage et la réactivité du zirconium et du Zircaloy-4 à haute température (de 450 °C à 550 °C) sous oxygène, PhD thesis, UTC Compiègne, 2003.
[8] I.M. Bernstein, Trans. Metall. Soc. AIME 239 (1967) 1518.
[9] T. Jacquot, R. Guillen, M. François, B. Bourniquel, J. Senevat, Mater. Sci. Forum 228–231 (1996) 845.
[10] L. Gaillet, Etude de la synergie déformation-oxydation lors du fluage d'un système Ni/NiO sous oxygène à 550 °C, Influence de la nature cristallographique du substrat de nickel et du mode d'élaboration de la couche d'oxyde NiO, PhD thesis, UTC Compiègne, 2000.
[11] P.L. Gruzin, V.S. Emelyanov, G.G. Ryabova, C.B. Federov, in: Second Int. Conf. Peaceful Uses of Atomic Energy, Geneva, 1958, p. 187.
[12] D. Kaddour, S. Frechinet, A.F. Gourgues, J.C. Brachet, L. Portier, A. Pineau, Scripta Mater. 51 (2004) 515.